DENDRITIC SOLIDIFICATION WITH TRIANGULAR FINITE ELEMENTS

P. Zhao*, M. J. Vénere[†], and J. C. Heinrich*

* Department of Aerospace and Mechanical Engineering
The University of Arizona
Tucson Arizona 85721, USA
e-mail: pzhao@u.arizona.edu; heinrich@zeus.ame.arizona.edu

[†] PLADEMA-CNEA
Universidad Nacional del Centro, Provincia de Buenos Aires
7000 Tandil, Argentina
e-mail: venerem@exa.unicen.edu.ar

Key Words: Finite Elements, Moving Boundaries, Dendritic Solidification

Abstract. The use of triangular elements in simulations of dendritic solidification of binary alloys is examined. The simulations require the solution of the diffusion equation for the solute concentration in very distorted geometries that change continuously with time, therefore a new mesh of triangular elements is generated at each time step and data from the previous mesh interpolated to the new one. It is shown that because of the exponential nature of the solute concentration field and the large number of time steps/interpolations, linear triangles suffer from excessive interpolation error that leads to unacceptable error in the total mass conservation unless unreasonably fine meshes are used. The problem is greatly alleviated by the use of quadratic triangles, which introduce the curvature needed to obtain better accuracy in the interpolation of the exponential fields. Examples of simulations of dendritic growth in binary alloys are given.

1 INTRODUCTION

The importance of understanding dendritic growth is critical to the manufacturing of high-temperature-resistant castings used in the aerospace industry and for the production of the high-quality crystals needed in the electronics industry. Numerical modeling of directional solidification of alloys requires the time integration of a moving boundary problem made unstable by constitutional undercooling. Moreover, in a typical alloy, such as the Pb-Sb model alloys used in this work, the thermal and solute diffusivities differ by four orders of magnitude, which makes these simulations, even today, a formidable challenge. In previous work it has been assumed that the solutions are very dilute,[1-5] or eutectic,[6,7] and that the temperature field is known, either constant or a prescribed gradient, in order to alleviate these difficulties. The latter assumption requires that the latent heat release be negligible, and it reduces the problem to the solution of the solute concentration in the liquid only. However, none of these assumptions is valid for high concentrations of solute.

In simulations of solidification of binary alloys the solute concentration in the liquid must be calculated in a domain that is continuously evolving and that can become topologically extremely complicated.[1,2,8,9] In most metallic alloys the solute diffusion coefficient in the solid is several orders of magnitude smaller than the diffusion in the liquid, which in turn is several orders of magnitude smaller than the heat diffusion; therefore solute diffusion in the solid is usually neglected. The solute diffusion in the liquid must then be calculated in a region that is complicated and continuously changing, placing severe demands on the generation of adequate computational meshes. In this work the problem has been addressed utilizing the mesh generation techniques developed in Refs. 10-12 based on triangular elements. The algorithm developed in Ref. 9 solves the energy equation over a fixed mesh of bilinear quadrilateral elements; the solid-liquid interface is tracked using a set of marker points that move according to the interface velocity and the number of markers can change to maintain a uniform resolution as the interface evolves.[8] The solute concentration in the liquid is solved independently on a variable mesh of triangular elements; a new triangular mesh is generated at every time step to follow the geometric change of the domain containing the liquid. The temperature and the solute concentration fields are coupled at the interface through a generalized Gibbs-Thompson equation.

The next section contains the mathematical model used in this work. Section 3 discusses the triangular interpolation schemes and the error associated with them and present numerical simulations of solidification. We close with a discussion in section 4.

2 GOVERNING EQUATIONS

We assume that the only transport mechanism in the solidification/melting process is diffusion, the material properties are different but constant in each phase, the latent heat is constant, and fluid flow is ignored so the densities must be equal in the solid and liquid. The energy equation is given by

$$\rho c_{PS} \frac{\partial T_S}{\partial t} = \kappa_S \nabla^2 T_S \qquad \text{in the solid} \qquad (1a)$$

and

$$\rho c_{PL} \frac{\partial T_L}{\partial t} = \kappa_L \nabla^2 T_L \qquad \text{in the liquid} \qquad (1b)$$

At the solid-liquid interface we must satisfy the conditions

$$T_S = T_L = T_I \qquad (2a)$$

and

$$(\kappa_S \nabla T_S - \kappa_L \nabla T_L) \cdot \hat{n} = \rho \left[L + (c_{PL} - c_{PS})(T_I - T_m) \right] V \qquad (2b)$$

In the above equations, the subscripts S and L denote the solid and liquid phases, respectively; ρ is the density; c_P is the specific heat; κ is the thermal conductivity; $\hat{n}$ is the unit vector normal to the interface pointing into the liquid; L is the latent heat; T_I and T_m are the local interface and equilibrium liquidus temperatures, respectively; and V is the local normal interface velocity. We also define the solid and liquid thermal diffusivities by $\alpha_S = \kappa_S / \rho c_{PS}$ and $\alpha_L = \kappa_L / \rho c_{PL}$, respectively.

Solute diffusion in the solid is neglected. The solute concentration is solved only in the liquid and is given by

$$\frac{\partial C_L}{\partial t} = D_L \nabla^2 C_L \qquad (3)$$

with interface conditions

$$(-D_L \nabla C_L) \cdot \hat{n} = (1 - k) C_L V \qquad \text{before eutectic} \qquad (4a)$$

and

$$C_L = C_E \qquad \text{at eutectic} \qquad (4b)$$

In Equations (3), (4a), and (4b), D_L is the solute diffusion coefficient in the liquid, k is the equilibrium partition ratio, and C_E is the eutectic concentration.

The local interface temperature is given by the generalized Gibbs-Thompson relation[13]

$$T_I - T_m + \frac{\gamma T_m}{L \rho} \mathbb{C} + \frac{V}{\nu} + \frac{T_m (c_{PL} - c_{PS})}{L} \left[T_I \ln\left(\frac{T_I}{T_m}\right) + T_m - T_I \right] = 0 \qquad (5)$$

where γ is the surface energy; $\mathbb{C}$ is the local interface curvature, and ν is the kinetic mobility. The liquidus of the phase diagram is approximated linearly by

$$T_m = T_{m0} + m C_L \qquad (6)$$

Here m is the slope of the liquidus line and T_{m0} is the melting point of the pure solvent.

The equations are solved using a standard Galerkin finite element formulation. The novelty of the approach is that the energy and solute conservation in the liquid are solved in separate independent meshes, and the mesh for the solute conservation equation changes at every time step as the solid-liquid interface advances. The solution algorithm has been explained in detail in Refs. 8 and 9 and will not be repeated here.

3 TRIANGULAR INTERPOLATION

Because of the complex morphologies that develop during the dendritic solidification process, the solution of the solute concentration equation in the liquid is obtained using meshes based on triangular elements. An example of one such mesh is shown in Figure 1. The mesh is extremely refined at and near the solid-liquid interface; this is necessary to resolve the new diffusion length scale given by $\ell_C = D_L/V$, which is much smaller than the thermal diffusion length scale $\ell_T = \alpha_L/V$. To be more specific, we will use the properties for Pb-Sb alloys listed in Table 1, where we see that D_L is four orders of magnitude smaller than α_L. This leads to very steep gradients of solute concentration at the solid-liquid interface that decay exponentially in the direction normal to the interface and must be resolved by the mesh. To illustrate the behavior of linear and quadratic triangles under these circumstances, let us first look at a one-dimensional example. With Equation (5) simplified to

$$T_I - T_m + \frac{V}{v} = 0 \tag{7}$$

due to the absence ofcurvature and neglecting the small contribution of the difference in specific heat. We consider a Pb-2.2 wt%Sb alloy using the properties in Table 1. The domain is 20 mm long. An initial temperature gradient of 10 K/mm is imposed and fixed at the right boundary, and a cooling rate of 0.1 K/s is applied at the left boundary. Simulations using graded meshes that initially contain 400 linear elements and 200 quadratic elements in the liquid region were done, with the elements near the interface refined so that the minimum distance between nodes was less than $0.2\ell_C$; these refined elements moved with the interface. A time step of 0.05 s was used, and during the simulation, at each time step, the total solute mass was calculated. The total number of time steps/interpolations in a simulation where 85% of the domain was solidified is approximately 26,000. The error in mass conservation as a function of the interface position is shown in Figure 2. It can be observed that by the time the interface reaches 5 mm the linear elements already show an error in mass conservation of about1.5%, which is unacceptable. On the other hand, the error for quadratic elements has not reached 0.7% after the interface has advanced 17 mm.
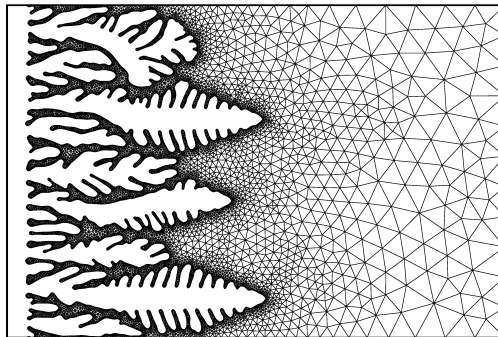
Figure 1. Morphology of dendritic growth and triangular finite element mesh that conforms to the interface.

Table 1. Physical properties of a Pb-Sb alloy.

Property	Symbol and Unit	Value
Bulk concentration of Sb	C_0, wt%	2.2
Solute diffusivity	D_L, mm^2/s	1.13×10^{-3}
Solute partition ratio	k	0.312
Eutectic concentration	C_E, wt%	11.2
Slope of liquidus line	m, K/wt%	-6.829
Melting temperature of pure solvent	T_{m0}, K	600.0
Eutectic temperature	T_E, K	523.5
Density	ρ, kg/mm^3	1.0416×10^{-5}
Specific heat of solid	c_{PS}, J/kg$\cdot$K	142.0
Specific heat of liquid	c_{PL}, J/kg$\cdot$K	151.0
Heat conductivity in the solid	κ_S, J/s$\cdot$mm$\cdot$K	0.030
Heat conductivity in the liquid	κ_L, J/s$\cdot$mm$\cdot$K	0.016
Latent heat of fusion	L, J/kg	29775
Surface energy	γ, J/mm^2	7.0×10^{-8}
Kinetic mobility	ν, mm/s$\cdot$K	6.67
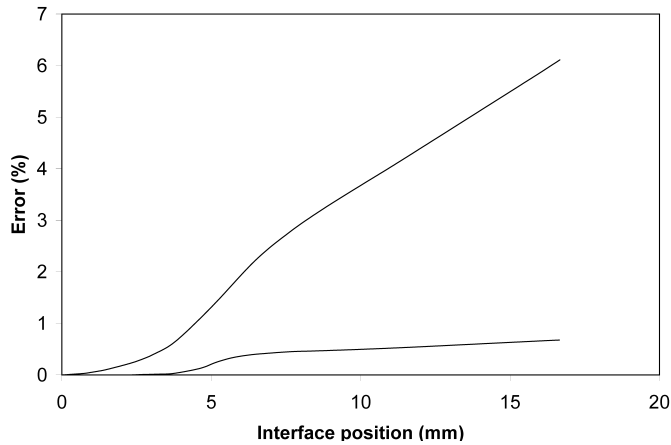
Figure 2. Mass conservation error vs. interface position for one-dimensional solidification of Pb-2.2wt%Sb.

Next we solve a one-dimensional problem in a two-dimensional domain using linear and quadratic triangular elements to compare their performance. As shown in Figure 3a, the domain is 10 mm by 1 mm. Initially the solute concentration is uniform with $C_L = C_0$, which is also the boundary condition at infinity. At time $t = 0$, the interface, which is the left-side wall, starts to move with a constant velocity V. Solidification proceeds as the interface moves to the right-hand side, and the solute concentration at the interface builds up due to the rejection of solute there. Under the assumptions that the interface is plane and that the solute diffusion in the solid can be ignored, the problem simplifies to a one-dimensional moving boundary diffusion problem. In a coordinate system moving with the interface it is governed by the convection-diffusion equation

$$\frac{\partial C_L}{\partial t} = D_L \frac{\partial^2 C_L}{\partial x^2} + V \frac{\partial C_L}{\partial x} \tag{8}$$

with interface condition

$$-D_L \frac{\partial C_L}{\partial x} = (1-k)C_L V \qquad \text{at } x = 0 \tag{9}$$

The time-dependent equation, (8), was solved analytically in Ref. 14. After the initial transient, the final steady state is

$$C_L = C_0 \left[1 + (1-k)e^{-xV/D_L} \big/ k \right] \tag{10}$$

Calculations were performed using two meshes, one of linear triangles with 41559 elements and 21234 nodes; the other with 4915 quadratic triangular elements and 10066 nodes. The ratio of the number of nodes in the two meshes is approximately 2:1, and that of the number of elements is 8:1. Calculations were carried out from the initial uniform state until the distribution of the solute concentration no longer changed. The calculated results were then compared with the analytical steady-state solution given in equation (10). The maximum relative error for various values of the steady-state velocity is shown in Figure 4. The errors are small for both meshes; however, it is clear that as the interface velocity increases the error in the linear elements grows very fast.
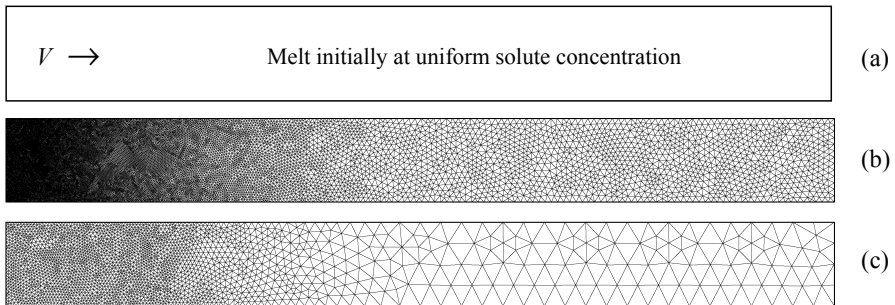
Figure 3. Domain and finite element meshes used to simulate solidification from a planar interface: (a) computational domain; (b) linear elements; (c) quadratic elements.
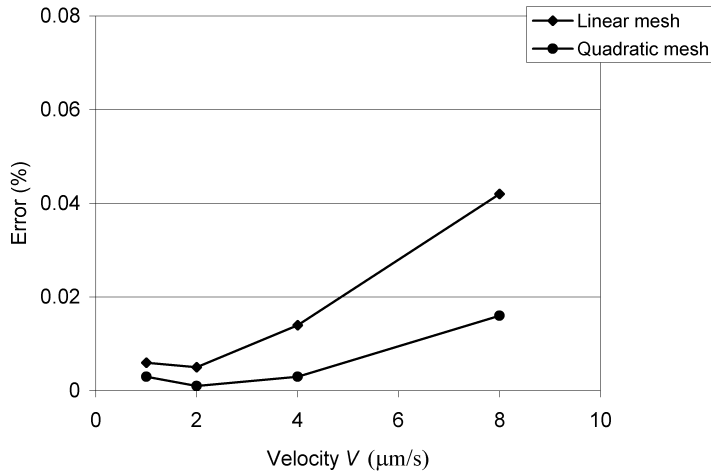
Figure 4. Accuracy of the solute concentration calculated using linear and quadratic meshes in Fig. 3. The error is the relative difference in the solute concentration with respect to the analytic solution, and V is the fixed interface velocity.

The last simulation involves cellular and dendritic growth of a Pb-Sb alloy from a planar front. We consider cellular growth from a perturbed plane front for a very dilute Pb-0.02wt%Sb alloy. The same problem was considered by Ungar and Brown[3] with an approximate model that solved only the solute concentration equation and found the position of the interface implicitly. Here the fully coupled equations, (1)-(6), are used in the simulation. The linear stability analysis of Mullins and Sekerka[15] predicts a preferred wavelength $\lambda^* = 0.1\,\text{mm}$ at the Péclet number $Pe = V\lambda^*/D_L = 1.0$ used in this calculation. To best approximate the conditions in Ref. 3 for comparison purposes, steady-state temperature and solute concentration fields are first calculated in one dimension. Starting with an initial temperature gradient $G = 1.008\,\text{K/mm}$ and the temperature at the left end $T(x=0) = T_m(C_0)$, at time $t > 0$ a cooling rate is applied at $x = 0$ and the initial temperature gradient is imposed in the right boundary. The domain is long enough to reach a steady state, and the cooling rate is adjusted to obtain $Pe = 1.0$. The steady-state solute and temperature fields obtained in this manner are used as initial conditions in the two-dimensional calculation, starting from a planar interface that is perturbed with a cosine perturbation with wavelength $\lambda^* = 0.1\,\text{mm}$ and amplitude $0.01\lambda^*$. The two-dimensional domain is chosen to be 2 by 0.6 mm so we expect six cells to develop. The mesh for the temperature solution has 100 by 30 bilinear elements and is the same for both types of triangles. The mesh of linear triangular elements contains approximately 10,000 nodes and 40,000 elements; the mesh of quadratic triangles ha approximately the same number of nodes and 10,000 elements. These meshes were chosen so that close to the interface the element's size does not exceed $0.2\ell_C$.

Figure 5 shows the error in the solute mass conservation as a function of time, using linear and quadratic triangles. The excessive error in linear elements is clearly observed. The results of the calculation with quadratic triangles after 60 s are shown in Figure 6. The expected six
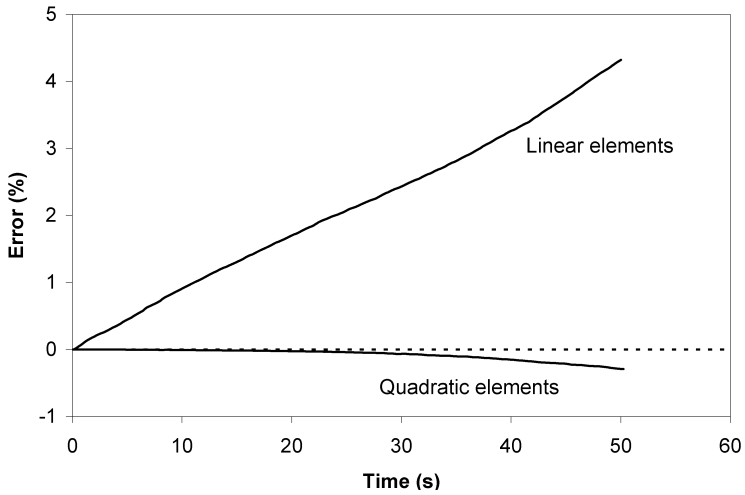
Figure. 5. Mass conservation error vs. simulation time for two-dimensional solidification of Pb-0.02wt%Sb.
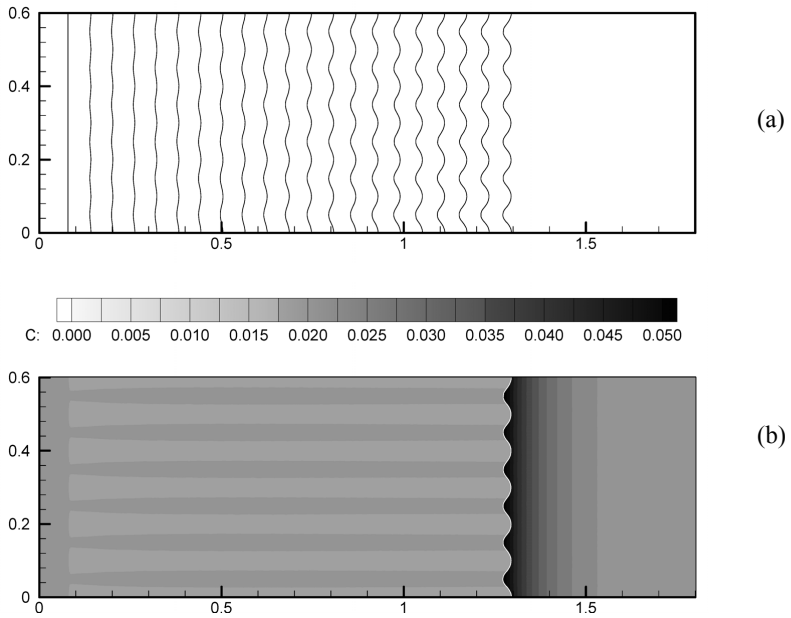
Figure 6. Solidification of Pb-0.02%wtSb from a perturbed plane front: (a) interface position at intervals of 3 s; (b) solute concentration at 60 s (the interface is white).

2831

cells develop and the expected microsegregation between cells can be observed. Finally, Figure 7 shows results of a calculation for Pb-0.2wt%Sb using quadratic triangles in a domain of 0.8 by 0.24 mm because at this concentration the preferred unstable wavelength is approximately 0.02 mm. A random perturbation was applied at the initially plane interface. In Figure 7a we observe that initially the instability grows very rapidly from small protuberances to a cellular morphology and then it becomes dendritic. Figure 7b shows the solute concentration after 4 s of simulation; considerable microsegregation is seen to be present.

4 CONCLUSION

Simulations of dendritic growth in binary alloys have been performed using a finite element model that solves the temperature and solute concentration equations in independent meshes. The mesh for the temperature is fixed throughout the calculation but the mesh for the solute concentration changes at every time step. The latter is based on triangular elements due to the complexity of the domain. We have shown that linear triangular elements cannot properly interpolate the exponentially decaying solute concentration field, and that they lead to excessive error in the mass conservation. Quadratic triangles, on the other hand, produce acceptable accuracy with meshes that are not overly refined. The method has produced the first calculations for solidification of binary alloys using the fully coupled equations of conservation of energy and solute.
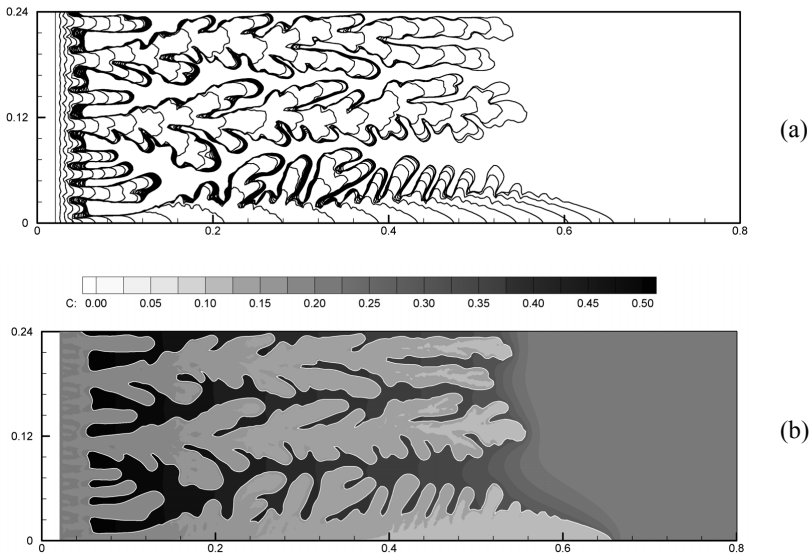
Figure 7. Solidification of Pb-0.2wt%Sb from a randomly perturbed planar front: (a) interface position at intervals of 0.2 second; (b) solute concentration at 4.0 seconds (the white line is the interface).

REFERENCES

[1]   A.A. Wheeler, W.J. Boettinger and G.B. McFadden, "Phase-field model for isothermal phase transitions in binary alloys," *Phys. Rev. A*, **45**, 7424-7439 (1992).

[2]   J.A. Warren and W.J. Boettinger, "Prediction of dendritic growth and microsegregation patterns in a binary alloy using the phase-field method," *Acta Metall. Mater.*, **43**, 689-703 (1995).

[3]   L.H. Ungar and R.A. Brown, "Cellular interface morphologies in directional solidification; IV. The formation of deep cells," *Phys. Rev. B*, **31**, 5931-5940 (1985).

[4]   G.B. McFadden, R.F. Boisvert and S.R. Coriell, "Nonplanar interface morphologies during directional solidification of binary alloys," *J. Cryst. Growth*, **84,** 371-388 (1987).

[5]   S.-Z. Lu and J.D. Hunt, "A numerical analysis of dendritic and cellular array growth: the space adjustment mechanism," *J. Cryst Growth*, **123**, 17-34 (1992).

[6]   A. Karma, "Phase-field model of eutectic growth," *Phys. Rev. E*, **49**, 2245-2250 (1994).

[7]   A.A. Wheeler, G.B. McFadden and W.J. Boettinger, "Phase-field model for solidification of a eutectic alloy," *Proc. Royal Soc.,* **452**, 495-525 (1996).

[8]   P. Zhao and J.C. Heinrich, "Front-tracking finite element method for dendritic solidification," *J. Comp. Phys.*, **173**, 765-796 (2001).

[9]   P. Zhao, M. Vénere, J.C. Heinrich and D.R. Poirier, "Modeling dendritic growth of a binary alloy*," J. Comp. Phys.* (submitted 2002).

[10] M.J. Vénere, "Técnicas adaptivas en cálculo numérico para problemas en dos y tres dimensiones," in *Mathématiques Appliquées aux Sciences de l'Ingenieur*,411-428, edited by C. Carasso, C. Conca, R. Correa and J.P. Puel, CÈDAPUÉS (1991).

[11] C. Padra and M.J. Vénere, "On adaptivity for diffusion problems using triangular elements," *Eng. Comput.*, **12**, 75-84 (1995).

[12] E.A. Dari and M.J. Vénere, "A node replacement method for automatic mesh generation," *Latin Amer. Appl. Res.*, **21**, 275-282 (1991).

[13] V. Alexiades and A.D. Solomon, *Mathematical modeling of melting and freezing processes*, p.106, Hemisphere Publishing Corp., Washington, DC (1993).

[14] V.G. Smith, W.A. Tiller and J.W. Dutter, "A mathematical analysis of solute redistribution during solidification," *Canadian J. of Physics*, **33**, 723-745 (1955).

[15] W.W. Mullins and R.F. Sekerka, "Stability of a planar interface during solidification of a dilute alloy," *J. Appl. Phys.*, **35**, 444-451 (1964).